A simulation model for crater formation in laser milling

T Dobrev, D T Pham and S S Dimov

Manufacturing Engineering Centre, Cardiff University, Cardiff, CF24 3AA

Abstract

In pulsed laser material removal systems, it is very important to understand the physical phenomena that take place during the laser ablation process. A two-dimensional theoretical model is developed to investigate the crater formation on a metal target by a microsecond laser pulse. The model takes into account the absorption of the laser light, and heating and vaporisation of the target, including an adjustment to compensate for the change of state. A simple numerical technique is employed to describe the major physical processes taking part in the laser milling process. The temperature distribution in the target material during the pulse duration is analysed. The effect of the laser fluence on the resulting crater is investigated in detail. The proposed simulation model was validated experimentally for laser material interactions between a microsecond Nd:YAG laser (λ= 1064 nm) and a stainless steel workpiece. The measured crater depths are in agreement with the model. Such a study is very important for understanding the mechanisms of micro-structuring when laser milling is employed. The results of this research will be used in improving the micro-machining capabilities of the process.

Keywords: laser milling, pulsed laser, microstructuring

1. Introduction

In pulsed laser material removal systems, it is very important to understand the physical phenomena that take place during the laser ablation process. The pulse duration and the relatively small material removal rates make an experimental investigation of all factors influencing the process difficult. Consequently, simulation models are considered important tools for a better understanding and optimisation of laser ablation parameters especially when laser milling is applied for machining micro features.

Many theoretical and experimental studies have been carried out on laser material heating and processing. The majority of mathematical models of the heat flow phenomena in laser material processing are based on the application of the classical heat conduction equation for stationary solids, applying the concept of an instantaneous heat source for an infinite volume. Cases with and without phase change and a variety of radiation or source conditions have been studied.

The aim of this research is to investigate the crater formation process in tooling materials resulting from irradiation with a microsecond laser pulse. Such a study is very important for understanding the mechanisms of micro-structuring when laser milling is employed. The results of this research will be used in improving the micro-machining capabilities of the process. In particular, a model of the crater formation is proposed to study the factors influencing the resulting surface finish. The model could be used as a tool to optimise the laser milling process for its broader use in a range of micro-structuring applications. For example, when laser milling is used in microtooling applications, the quality of the machined surfaces influences significantly the replication capabilities of the tools. The sequence of single craters formed on the surface determines its final topography.

This paper reports a simulation model that was developed to investigate the influence of a number of laser ablation parameters on temperature distribution, heat flow, material removal (e.g. resulting craters on the surface) and general laser/material interaction during a microsecond laser pulse irradiating a metal target.

2. Theoretical model

The developed model is based on the conventional heat diffusion equation with a heat source, a laser pulse with Gaussian temporal and spatial profiles. The model takes into account the relation between temperature and energy density, and the material change of state. However, the heat diffusion in the gas phase of the material is ignored because it is assumed that the liquid-to-gas transition removes material.

The general 2D heat conduction equation is employed in this research [1]:

$$\rho C_P \frac{\partial T(x,z,t)}{\partial t} = k\left(\frac{\partial^2 T}{\partial x^2} + \frac{\partial^2 T}{\partial z^2}\right) + A(x,z,t) \qquad (1)$$

where ρ is the density of the material [kg/m^3]; C_p – specific heat capacity [J/kgK]; k – thermal conductivity [W/mK]; x, z – space domain dimensions [m] (see Fig. 1); T – temperature [K]; t – time variable [s].

The term A(x, z, t) is the volume heat source (the absorbed laser energy in a given unit of a material volume):

$$A(x,z,t) = \alpha \times I_0 \times p(t,x) \times e^{-\alpha z} \qquad (2)$$

where I_0 is the peak on-line laser intensity [Wm^{-2}] and α is the absorption coefficient [m^{-1}] for the sample material. The term p(t, x) refers to the temporal and spatial geometry of the laser pulse, which is assumed to be Gaussian in both domains. The peak laser intensity I_0 is:

$$I_o = \frac{Peak\_Power}{Area} = \frac{P_{peak}}{\pi R_0^2} = \frac{E_p}{\tau\pi R_0^2} = \frac{P_{av}}{f\tau\pi R_0^2} \quad (3)$$

where f is the laser pulse frequency (repetition rate) [kHz], τ - pulse duration [s], E_p – pulse energy [J] and R_0 – the radius of the laser beam spot at the focus [μm].

3. Numerical solution of the heat equation

To investigate the influence of process parameters during laser machining of metal micro-structures the forward finite-difference method is applied [1]. Developing the general heat equation (1) in this way results in:

$$\frac{\partial T}{\partial t} = D\left(\frac{\partial^2 T}{\partial x^2} + \frac{\partial^2 T}{\partial z^2}\right) + \frac{D}{k}A(x,z,t) \quad (4)$$

where D is the thermal diffusivity of the target material [m^2s^{-1}] that is equal to:

$$D = \frac{k}{\rho C_p} \quad (5)$$

By applying the forward finite difference approximations of the derivatives to (4) and making the assumptions given in Table 1 the temperature $T_{i+1,j,k}$, can be calculated:

$$T_{i+1,j,k} = T_{i,j,k}\left(1 - 2\frac{\Delta tD}{\Delta x^2} - 2\frac{\Delta tD}{\Delta z^2}\right) + \Delta tD \times \left[\frac{(\Delta z)^2\left(T_{i,j+1,k} + T_{i,j-1,k}\right) + (\Delta x)^2\left(T_{i,j,k+1} + T_{i,j,k-1}\right)}{\Delta x^2 \Delta z^2}\right] + \frac{\Delta tD}{k}\alpha I_0 p(t,x) e^{-\alpha\left(z_k - h_j\right)} \quad (6)$$

Table 1 Assumptions for the numerical solution

Dimension	Index	Step	Number of steps
Time *t*	i	Δt	n_t
Axis *x*	j	Δx	n_x
Axis *z*	k	Δz	n_z

Equation (6) is *explicit* because the known temperatures at the previous time step determine unknown temperatures for the next time step *i+1*. In this way, the transient temperature distribution is obtained by iteration in time, in steps of Δt.

The distribution of the laser power in direction *x* and time *t* is assumed to be Gaussian and is given by:

$$p(t,x) = \int_{-\infty}^{\infty} e^{-\left(\frac{x}{R_0}\right)^2} dx \int_0^{\infty} e^{-\left(\frac{t}{\tau}\right)^2} dt \quad (7)$$

In order to solve this parabolic equation, an initial condition and three boundary conditions are required. At time 0, it is assumed that the temperature of the material is uniform and is equal to:

$$T(0,x,z) = 293K$$

The three boundary conditions apply constraints to the temperature with respect to the space domain:

$$T(t, x \to -\infty, z) = 293K$$
$$T(t, x \to +\infty, z) = 293K$$
$$T(t, x, z \to -\infty) = 293K$$

An undesirable characteristic of the explicit solution is that it is not unconditionally stable. In a transient problem, the solution for the nodal temperatures should continuously approach final, steady-state values with increase of time. However, the iterative nature of the explicit method could induce numerical oscillations, thus causing the solution to deviate from the actual result. To prevent this, the value chosen for Δt must be below a certain limit, which depends on Δx and other system parameters. This limit is called a *stability criterion*, and can be obtained mathematically [1]. Applying the stability criterion to (6) results in:

$$1 - 2\frac{\Delta tD}{\Delta x^2} - 2\frac{\Delta tD}{\Delta z^2} \geq 0 \quad (8)$$

Therefore, the largest time increment is:

$$\Delta t \leq \frac{1}{2}\frac{\rho C_p \Delta x^2 \Delta z^2}{k\left(\Delta x^2 + \Delta z^2\right)} \quad (9)$$

Transitions between solid, liquid, and gaseous phases involve large amounts of energy compared to the specific heat required for each change of state [2]. If heat is added at a constant rate to the material to take it through its phase changes from solid to liquid and then from liquid to gas states, the energies required to accomplish the phase changes (called the latent heat of melting L_m and latent heat of vaporization L_v) would lead to plateaux in the temperature T [K] vs time t [s] graph.

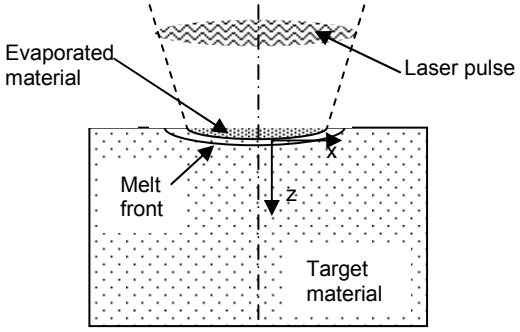

Fig. 1 Assumptions about the simulation spatial domain

Thus, in the simulation when a simulation cell reaches the melting point of the considered target material, the following temperature adjustment is introduced:

$$T_{new} = T_{old} - \frac{L_m}{C_p} \quad (10)$$

In the proposed model, the heat diffusion in the gas phase is not taken into account, because an assumption is made that the evaporated material is removed from the system. If a cell reaches sufficient energy density to vaporise its temperature is set to the melting temperature for the given

material [3]. Thus, in subsequent calculations, for their adjacent cells, such cells are ignored because they are considered as possible heat sources/sinks. Also the model disregards them as an absorption material, and the energy is delivered without loss to the next "layer" of cells.

4. Simulation results

Based on the proposed model, simulation software was developed in C++. The simulated laser source is representative of pulses generated from a Nd:YAG laser (λ = 1064 nm) with an intensity that has Gaussian time and space profiles. The pulse duration was assumed to be τ = 10 μs. The origin of the time axis (t = 0 s) was set in such a way that the maximum laser intensity occurred at t = 0.5τ, i.e. the beginning of the pulse and the start of the simulation coincided. The calculation times and the accuracy of the results are highly dependent on the temporal and spatial increments specified during the execution of the software. Thus, taking into account the trade-offs between the time and the accuracy required to validate the model, the following values were used for all simulation runs:

- Increment in *x* direction Δx = 2 μm
- Increment in *z* direction Δz = 0.4 μm
- Time step $\Delta t = 1 \times 10^{-8}$ s

It is worth noting the different spatial increments in *x* and *z*. This was due to the expected results. In particular, the estimated depth in *z* was expected to be in the range of 2 to 8 μm while the diameter of the crater along the *x* axis was anticipated to be between 40 and 80 μm.

Table 2 summarises the physical, optical and thermal properties of stainless steel 316, which were used in the simulations.

Table 2 Stainless steel Grade 316 material properties [1, 4, 5]

Property	Value	Units
Melting point, T_m	1670	K
Boiling point, T_v	3173	K
Density, ρ	8238	kg/m^3
Specific heat capacity, C_p	468	J/kgK
Thermal conductivity, *k*	13.4	W/mK
Thermal diffusivity, D	3.48×10^{-6}	m^2/s
Latent heat of melting, L_m	300	kJ/kg
Absorption coefficient @ 1064 nm	5.45×10^{7}	m^{-1}

Fig. 2 shows the evolution of the temperature in *z* direction and time when the laser fluence of a single pulse is 2.86 Jcm^{-2}. It is evident from this figure, that the target material starts melting before t = 3 μs, and the material evaporation begins at t = 4 μs. The flat area on the graphs indicates that the material removal through evaporation has already started. The depth of the crater increases until t = 8 μs reaching its maximum value of 6.8 μm. At that point the temperature starts decreasing, due to the cooling down of the melted material and even its solidification before the end of the pulse. Nevertheless, the crater depth is maintained and does not decrease because of the assumption that the material is removed completely from the interaction area.

Fig. 3 shows the resulting crater depth when the laser fluence is varied. The lowest value of the laser average power applied in the simulations corresponds to F_0 = 0.76 Jcm^{-2}. However, the crater depth for this power level is not shown in the figure, because the applied energy is not sufficient for the material to reach the evaporation temperature during the pulse. Above this threshold, the model predicts a proportional increase of the crater depth with the increase of the average laser fluence.

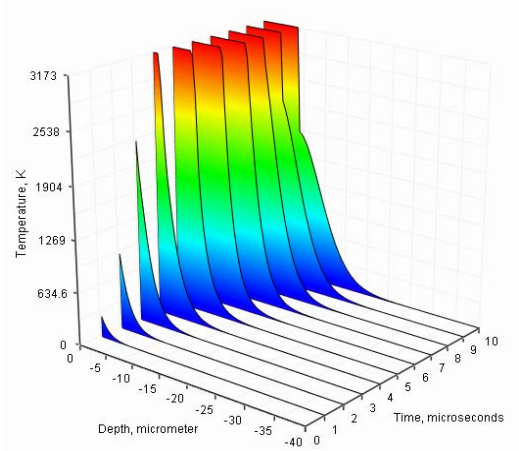

Fig. 2 Temperature distribution along the *z* axis for a laser fluence of 2.86 J/cm^2

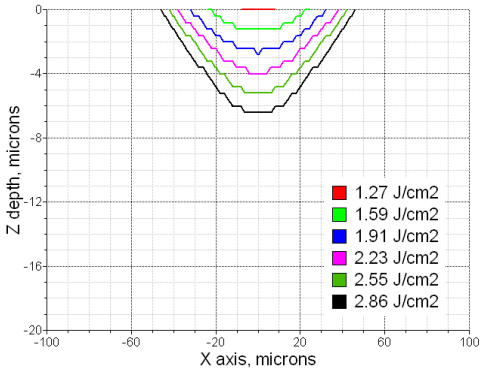

Fig. 3 Simulation crater depths obtained by varying the laser fluence

The experimental validation of the proposed simulation model is presented in the next section.

5. Experimental validation

All experiments were performed on an Nd:YAG (FOBA Laser F 94S) laser ablation system with a wavelength of 1064 nm and a pulse duration set to 10 μs. The average laser power delivered from the laser to the workpiece was measured with a laser power meter equipped with a high-power laser sensor [6] suitable for different laser flashlamp current levels and varying pulse frequencies.

The experiments were carried out on a single Grade 316 stainless steel workpiece. Initially the work surface was polished to achieve a very good surface finish, and then in order to decrease the reflection of the laser light from the top surface, it was matted.

After completing the experiments, the workpiece was cleaned in an ultrasonic cleaning

bath, to remove any contamination and debris from the surface. Then the 3D surface profiles of any 3 craters from each set of experiments were measured using white light interferometry equipment (MicroXAM). Fig. 4 shows the 3D profile of one of the measured craters. This crater was produced with an operational laser fluence F_0 = 2.56 Jcm^{-2}. Its average depth is d_m = 4.65 μm, while the simulation results for the same laser fluence predicted a crater with a depth of 5.1μm (see Fig. 5).

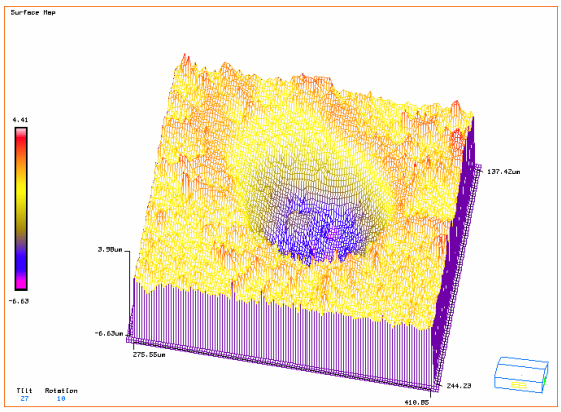

Fig. 4 3D profile of a single crater

Fig. 5 compares the ablation depth predicted using the simulation software with that of the craters produced during the experiments. For a laser fluence above 2.5 Jcm^{-2} there is a good agreement of the simulation results with those from the experiments. There is a significant difference though between the ablation threshold value, predicted from the model of around F_0 = 0.76 Jcm^{-2}, and that observed during the experiments, of F_0 = 0.36 Jcm^{-2}. However, it should be noted that the removed material was within or less than the depth increment (Δz = 0.4 μm) used in the model.

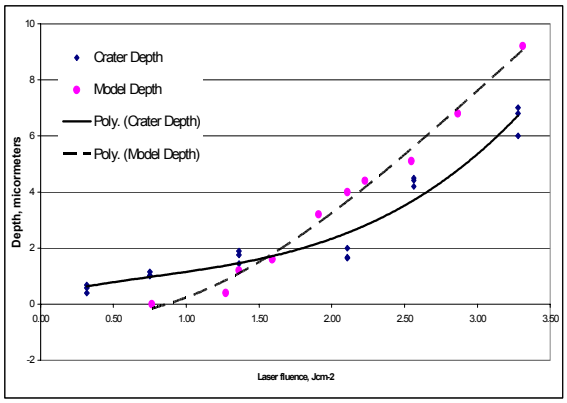

Fig. 5 Model predictions and measured crater depths

It can be seen in Fig. 5 that at a high and a low fluence the model predicts that more or less material would be evaporated from the target respectively. This could be explained by the simplified absorption process that takes place during the material evaporation. The more material is evaporated, the more energy is absorbed into it, thus letting a smaller amount of energy to reach the target surface.

6. Conclusions

The paper presents a simulation model developed to investigate the crater formation during the laser milling of metal targets. A simple numerical solution is proposed for the heat conduction equation with a volume heat source representing a laser pulse with Gaussian temporal and spatial profiles. The model takes into account the following process characteristics:

- Target absorption of the incident laser pulse
- Heat diffusion into the bulk material
- Temporal and spatial pulse shape (Gaussian)
- Material phase transition from solid to liquid to gas state

The proposed simulation model was validated experimentally for laser material interactions between a microsecond Nd:YAG laser (λ= 1064 nm) and a stainless steel workpiece. The depth of the craters produced during the experiments are in good agreement with that predicted by the model especially for a laser fluence above 2.5 Jcm^{-2}.

The model can be used to study the factors influencing the resulting surface finish after laser milling, it is also a good tool for process optimisation especially when laser ablation is used for micro-structuring.

Acknowledgements

The authors would like to thank the UK Engineering and Physical Sciences Research Council for funding this research under the EPSRC Programme "The Cardiff Innovative Manufacture Research Centre". Also, this work was carried out within the framework of the EC Network of Excellence "Multi-Material Micro Manufacture: Technologies and Applications (4M)".

Reference

[1] Incropera F P. *Fundamentals of heat and mass transfer* / Frank P. Incropera, David P. DeWitt., ed. 5. New York : J. Wiley, 2002

[2] Smurov I Y, Uglov A A, Lashyn A M, Matteazzi P, Covelli L and Tagliaferri V. *Modelling of pulse-periodic energy flow adtion on metallic materials*. Int. J. Heat Mass Transfer, Vol. 34, No 4/5, 1991, pp. 961 – 9

[3] Nantel M, Yashkir Y, Lee S K, Mugford C, and Hockley B S. *Laser micromachining of semiconductors for photonics applications*. Proceedings of SPIE - Vol 4594, October 2001, pp. 156-167

[4] Nath A K, Sridhar R, Ganesh P and Kaul R. SADHANA - India, Vol. 27, Part 3, June 2002, pp. 383 – 392

[5] Weaver JH, Krafka C, Lynch D W and Koch E E. *Optical properties of metals, Vol. I and Vol. II.* Zentralstelle für Atomkernenergie-Dokumentation, ZAED, 1981

[6] COHERENT, 2004. [WWW]: Power meter: Coherent FieldMaster GS; Power sensor: Coherent LM200 HTD – http://www.coherentinc.com/